# Load Balancing-based Topology Adaptation for Integrated Access and Backhaul Networks

Raul Victor de O. Paiva, Fco. Italo G. Carvalho, Fco. Rafael M. Lima, Victor F. Monteiro, Diego A. Sousa, Darlan C. Moreira, Tarcisio F. Maciel and Behrooz Makki

***Abstract*—Integrated access and backhaul (IAB) technology is a flexible solution for network densification. IAB nodes can also be deployed in moving nodes such as buses and trains, i.e., mobile IAB (mIAB). As mIAB nodes can move around the coverage area, the connection between mIAB nodes and their parent macro base stations (BSs), IAB donor, is sometimes required to change in order to keep an acceptable backhaul link, the so called topology adaptation (TA). The change from one IAB donor to another may strongly impact the system load distribution, possibly causing unsatisfactory backhaul service due to the lack of radio resources. Based on this, TA should consider both backhaul link quality and traffic load. In this work, we propose a load balancing algorithm based on TA for IAB networks, and compare it with an approach in which TA is triggered based on reference signal received power (RSRP) only. The results show that our proposed algorithm improves the passengers worst connections throughput in uplink (UL) and, more modestly, also in downlink (DL), without impairing the pedestrian quality of service (QoS) significantly.**

***Index Terms*—mIAB, topology adaptation, load balancing.**

## I. Introduction

The use of the large available bands in millimeter wave (mmWave) frequencies in fifth generation (5G) networks allows the fulfillment of quality of service (QoS) requirements for new data-hungry services. However, that part of the spectrum suffers from severe path and penetration losses [1], [2]. To overcome these drawbacks, one envisioned solution is the densification of the network with integrated access and backhaul (IAB) nodes.

In summary, an IAB node can be seen as a regular gNodeB (gNB) in which the backhaul is wireless, being served by another network node, called IAB donor. IAB nodes enable deploying new infrastructure avoiding the high costs and time consumption of traditional wired installations and overcoming possible limitations on trenching, such as in historical places [3]–[6].

In Release 18 [7], applications and technical requirements were investigated for 5G networks that use vehicle-mounted relays (VMRs) that provide service to onboard passengers and surrounding pedestrians. Additionally, VMRs are designed to facilitate seamless connectivity despite the mobility of the user equipments (UEs) and the VMR itself. For IAB networks, VMRs can be identified as mobile IAB (mIAB) [7].

Topology adaptation (TA), in this context, refers to the migration of an IAB node from an IAB donor to another one, which is triggered when the link between an IAB node and its current donors weakens, due to mobility and/or obstacles [8]. As mIAB nodes move, the traffic load in the system becomes more dynamic and heterogeneous. Specifically, in a given instant of time, one macro base station (BS) may serve only a few pedestrians, while other macro BSs may serve several mIAB nodes through their backhaul as well as direct pedestrians. Thus, depending on the system load distribution, not all IAB donors can provide satisfactory backhaul service to a coming mIAB node, due to the lack of available radio resources.

The authors in [9] surveyed several works on IAB and mIAB and presented a detailed performance evaluation in order to assess the gains of mIAB over conventional deployments. It was shown that the load variability among IAB donors is in general high with mIAB nodes. The authors then discussed the need of TA strategies that consider IAB donor load to avoid overloading IAB donors.

In [10], the authors proposed a method to distribute the load among fixed IAB nodes efficiently by sharing their load information and data processing capabilities. The proposed method outperformed traditional approaches based on metrics such as reference signal received power (RSRP) in terms of average throughput and number of served UEs. In [11], it is proposed a graph-based load-balancing algorithm for small-cell IAB networks in the mmWave band which addresses the issue of unbalanced load distribution across BSs. However, a multi-hop of fixed IAB scenario is considered. Motivated by the conclusions of [9]–[11] and use cases involving load

Raul Victor de O. Paiva is with the Wireless Telecommunications Research Group (GTEL), Federal University of Ceará (UFC), Fortaleza - Ceará - Brazil; e-mail: raul.paiva@gtel.ufc.br; ORCID: 0009-0005-6453-6239. Fco. Italo G. Carvalho is with GTEL, UFC, Fortaleza - Ceará - Brazil; e-mail: italoguedes@gtel.ufc.br; ORCID: 0009-0009-2033-9902. Francisco R. M. Lima is with GTEL, UFC, Fortaleza - Ceará - Brazil and with UFC - Campus Sobral, Sobral - Ceará - Brazil; e-mail: rafaelm@gtel.ufc.br; ORCID: 0000-0002-4115-1935. Victor F. Monteiro is with GTEL, UFC, Fortaleza - Ceará - Brazil; e-mail: victor@gtel.ufc.br; ORCID: 0000-0002-6462-4686. Diego A. Sousa is with GTEL, UFC, Fortaleza - Ceará - Brazil and with the Federal Institute of Education, Science, and Technology of Ceará (IFCE), Paracuru - Ceará - Brazil; e-mail: diego@gtel.ufc.br; ORCID: 0000-0001-9737-4882. Darlan C. Moreira is with GTEL, UFC, Fortaleza - Ceará - Brazil; e-mail: darlan@gtel.ufc.br; ORCID: 0000-0002-2199-3748. Tarcisio F. Maciel is with GTEL, UFC, Fortaleza - Ceará - Brazil; e-mail: maciel@gtel.ufc.br; ORCID: 0000-0002-8861-1708. Behrooz Makki is with Ericsson Research, Sweden. ORCID: 0000-0001-7863-997X.

This work was supported by Ericsson Research, Sweden, and Ericsson Innovation Center, Brazil, under UFC.51 Technical Cooperation Contract Ericsson/UFC. The work of Victor F. Monteiro was supported by CNPq under Grant 308267/2022-2. The work of Tarcisio F. Maciel was supported by CNPq under Grant 312471/2021-1. The work of Francisco R. M. Lima was supported by FUNCAP (edital BPI) under Grant BP4-0172-00245.01.00/20.
Submission: 2024-09-11, First decision: 2024-12-12, Acceptance: 2025-06-17, Publication: 2025-07-07.
Digital Object Identifier: 10.14209/jcis.2025.5

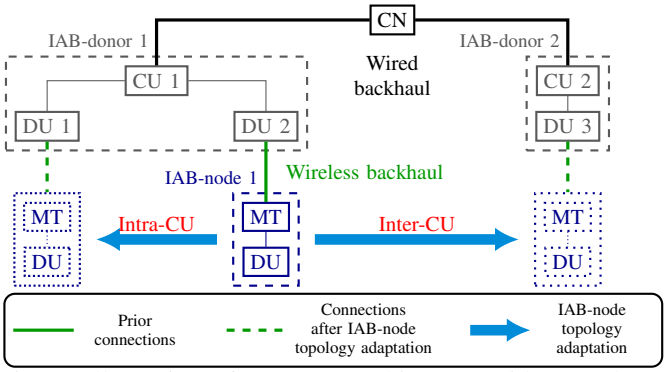


Fig. 1: Illustration of IAB NR architecture with IAB donor and nodes main components and topology adaptation [9].

balancing in Release 18 [7], we investigate load balancing based TA for mIAB in this paper.

In this letter, we propose a TA strategy that takes into account not only the channel strength but also the system load in a mIAB network. Results show that our proposed solution outperforms the standard TA solution, leading to improved throughput for passengers without significantly deteriorating the pedestrians' QoS.

## II. Mobile Integrated Access and Backhaul

The IAB architecture, illustrated in Fig. 1, was designed to support multiple wireless backhaul hops in new radio (NR). Therein, the blue boxes represent the IAB nodes. These nodes can connect to each other wirelessly. The IAB donors, shown as gray boxes, have a wired backhaul and provide wireless backhaul to an IAB node.

The IAB nodes can be split into distributed unit (DU) and mobile termination (MT) [12]. The MT component is responsible for managing the radio signal used to connect to a parent node that can be an IAB donor or an IAB node. The DU component serves as the NR interface for both UEs and the MT part of a child IAB node. The IAB donors, with wired backhaul to the core network (CN), have two parts: centralized unit (CU) and DU. Lower protocol layers are responsibility of the DUs, while the upper protocol layers are provided by the CUs [12]. The aforementioned split permits time-critical functionalities to be conducted in the DU near the served nodes, while others are handled with more processing power in the CU [4].

Wireless backhaul allows for the deployment of mobile cells, the mIAB nodes, that can provide uninterrupted cellular services for moving UEs [9]. The main use cases for mIAB technology consist in the service provision for both passengers onboard and pedestrians in the adjacency of the vehicle [7]. For buses, the outer antennas on top correspond to the MT, while the inner antennas correspond to the DU.

Concerning TA, an IAB node might need to switch to a different parent node after initial setup. This can happen, for example, if the connection to its current parent weakens due to movement or obstructions between them [8]. In fixed IAB scenarios, TA due to poor channel quality is less frequent, as nodes are stationary and well planned. In contrast, in mIAB scenarios, TA mainly occurs due to channel variations caused by the movement of transmitters and receivers [8].

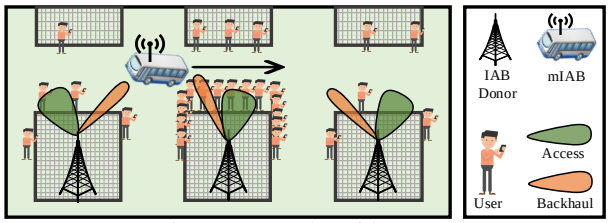


Fig. 2: Scenario of interest.

Figure 1 shows a TA illustration for IAB node 1 in a scenario with two IAB donors (donors 1 and 2) . Assuming IAB node 1 as an mIAB, we can see that it has donor 1 (through DU 2) as parent node and needs to switch to another parent node due to poor backhaul link quality. Donor 1 (through DU 1) and donor 2 are candidate parent nodes. In this case, donor 1 through DU 1 may provide a connection with the same IAB donor-CU (intra-CU), while donor 2 may provide a different IAB donor-CU (inter-CU). The inter-CU case involves handover requests [8].

## III. System Model and Load-Aware Topology Adaptation

In Fig. 2, the proposed study scenario is shown. It considers a single bus equipped with an mIAB, which is connected to an IAB donor and, as the time passes, gets closer to two other donors, the closest (center) one being overloaded.

Conventionally, the mIAB node performs TA to the IAB donor that provides the strongest backhaul link quality, e.g., highest RSRP, which is usually the closest one. However, in the considered scenario, the choice of the IAB donor with stronger RSRP may degrade the connection of onboard UEs, since the the closest IAB donor is overloaded. Thus, few radio resources would be left for backhaul connection.

A solution for this situation is to avoid the connection of the incoming mIAB node to the overloaded IAB donor and, eventually, connecting it to another, less loaded, IAB donor instead. The following Algorithm 1 is proposed to this end. It selects an IAB donor for the mIAB node considering both the backhaul link quality and the traffic load of the candidate donors. It iterates through all potential IAB donors and checks their suitability based on three main conditions. Let $D$, $P$ and $C$ be the IAB donor, parent and candidate, respectively. The variables $C_{bits}$ and $P_{bits}$ denote the amount of buffered bits at the candidate and parent IAB donors, respectively. Analogously, $C_{RSRP}$ and $P_{RSRP}$ denote the link metric (RSRP) estimated on pilot signals of the candidate and parent IAB donors, respectively. First, the candidate donor must have a lower traffic load (in bits) than the current serving donor (line 3), ensuring that the new connection does not worsen congestion at the newly selected donor. Second, the candidate donor must provide a backhaul link with an RSRP higher than a predefined threshold ($min_{RSRP}$) (line 4), guaranteeing a minimum level of signal quality. Third, the RSRP of the candidate donor must not be much lower than that of the current donor (line 5) considering a hysteresis offset ($\Delta(min_{RSRP})$), as to prevent unnecessary handovers due to small fluctuations in signal strength. If a candidate donor satisfies all these conditions, it is selected as the new

parent IAB donor for the mIAB node. This approach avoids connecting to the nearest, potentially overloaded donor and instead balances the load across available donors, improving the overall efficiency of the network. The buffer occupancy information is updated every transmission time interval (TTI), which is set to 0.25 ms. The algorithm for updating the donor choice is executed when all the conditions specified in the algorithm are satisfied within a time-to-trigger (TTT) of 40 ms. When multiple mIABs are present in the scenario, the donor evaluates both the RSRP and the current load of each mIAB before making a handover decision. This coordinated evaluation should prevent several mIABs from simultaneously migrating to the same lightly loaded donor, thus avoiding potential overload and instability.

The main objective of this work is to compare a standard TA algorithm [9] which considers only the RSRP value as activation criterion, hereafter called standard algorithm, against the proposed Algorithm 1.

## IV. Practical Implementation Aspects

To support the execution of the proposed algorithm in a practical 5G IAB scenario, a signaling framework is assumed wherein IAB donors periodically exchange load-related information, i.e., buffer occupancy levels, with one another. This exchange allows each IAB donor to maintain a network-wide view of the load distribution across all donor nodes, enabling informed decision-making. Simultaneously, both UEs and mIAB nodes transmit control messages to their serving IAB donor. Among these, the Buffer Status Report (BSR) is a MAC Control Element used to report the amount of uplink (UL) data awaiting transmission. Additionally, the Measurement Report (MR) is employed by UEs and mIABs to provide the serving node with radio link quality measurements toward neighboring cells. In the simulation environment, both the inter-donor buffer status exchange and the reception of BSRs and MRs occur at each slot, and the donor-side algorithm is likewise executed on a per-slot basis. This periodic exchange of information ensures that donor nodes can react promptly to changes in network load and link quality, which is essential for real-time operation in dynamic scenarios.

In practical deployments, challenges such as simultaneous donor selection by multiple mIAB nodes and potential decision oscillations may arise due to synchronized information and similar network conditions. Although not explicitly addressed in the current algorithm, such effects can be mitigated through mechanisms like randomized decision timers, migration thresholds, or hysteresis, which are left as directions for future work.

**Algorithm 1:** Update parent IAB donor ($P$)

**Input:** List of IAB donors: $\mathbf{D}$
**Output:** Updated parent IAB donor: $P$

```
foreach C in D do
    if C is not P then
        if C_bits < P_bits then
            if C_RSRP > min_RSRP then
                if C_RSRP > P_RSRP - Δ(min_RSRP) then
                    P ← C;
```

TABLE I: Entities characteristics.

| Parameter | IAB donor | mIAB node | | UE | |
|---|---|---|---|---|---|
| | | DU | MT | Ped. | Pass. |
| Height | 25 m | 2.5 m | 3.5 m | 1.5 m | 1.8 m |
| Transmit power | 35 dBm | 24 dBm | 24 dBm | 24 dBm | 24 dBm |
| Antenna tilt | 12° | 4° | 0° | 0° | 0° |
| Antenna type | 64 ULA | 8 × 8 URA | 64 ULA | Single | Single |
| Antenna element pattern | 3GPP [15] | 3GPP [15] | Omni | Omni | Omni |
| Max. antenna element gain | 8 dBi | 8 dBi | 0 dBi | 0 dBi | 0 dBi |
| Speed | 0 km/h | 50 km/h | 50 km/h | 3 km/h | 50 km/h |

TABLE II: Simulation parameters.

| Parameter | Value |
|---|---|
| Layout | Simplified Madrid grid [13], [14] |
| Carrier frequency | 28 GHz |
| Subcarrier spacing | 60 kHz |
| Number of subcarriers per RB | 12 |
| Number of RBs | 22 |
| Slot duration | 0.25 ms |
| OFDM symbols per slot | 14 |
| Channel model | Stochastic model by [16] |
| Channel generation procedure | As described in [15, Fig. 7.6.4-1] |
| Path loss | As described in [15, Table 7.4.1-1] |
| Fast fading | As described in [15, Sec.7.5] and [15, Table 7.5-6] |
| AWGN power per subcarrier | −174 dBm |
| Noise figure | 9 dB |
| Mobility model | Pedestrian and Vehicular [17] |
| Number of buses | 1 |
| Passengers + pedestrians | 56 |
| CBR traffic packet size | 4, 096 bits |
| CBR traffic packet inter-arrival time | 4 slots |
| TTT | 40 ms |
| $min_{RSRP}$ | −1000 dBm |
| $\Delta(min_{RSRP})$ | 0 dB |
| Independent runs | 40 runs |

## V. Performance Evaluation

This section presents a performance comparison between the standard and the proposed TA algorithms. The main simulation parameters are presented in subsection V-A and the results are discussed in subsection V-B.

### A. Simulation Assumptions

The considered scenario of interest, presented in Fig. 2, has one bus that serves 6 passengers through its IAB node, which is traveling with a constant speed of 50 km/h on a trajectory that passes in front of 3 building blocks modeled using a simplified Madrid Grid [13], [14]. One IAB donor is placed at the end of the opposing side of each block, from where the IAB node passes. 40 pedestrians moving with a speed of 3 km/h are connected to the central IAB donor, while the other IAB donors serve only 5 pedestrians, each. We consider 22 resource blocks (RBs), that are shared by all the network nodes. Also, a constant bit rate (CBR) traffic model is assumed, generating packets with size 4.096 bits each 1 ms. The values of the simulation parameters are presented in Tables I and II.

In order to avoid self-interference, IAB-DU and IAB-MT operate in half duplex (HD), meaning that one cannot transmit while the other is receiving, i.e., they operate together in the same direction, either both transmitting or receiving.

It is worth noting that link quality measurements of a candidate IAB donor are performed on the same pilot signals used to estimate link quality metrics, such as RSRP. These pilots are not affected by interference due to load, being the

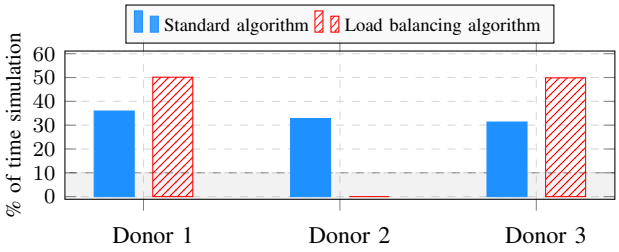


Fig. 3: Total time the mIAB remains connected with donors 1, 2 and 3 with the standard and load balancing algorithms.

noise perceived on them the same as in any other channel and not influenced by load.

### *B. Simulation Results*

This section presents the simulation results in terms of mIAB node connection time, transmission buffer load, and throughput.

#### *B.1 mIAB node connection time*

In Fig. 3, we present the total time the mIAB node (bus) is connected with each IAB donor, with and without usage of the proposed the load balancing TA. We can see that using the standard TA algorithm [9], the mIAB node remains connected to each IAB donor approximatelly 33% of the simulation time, as expected considering the IAB node constant speed and the grid symmetry. When Algorithm 1 is used, there is no connection between the mIAB node and the overloaded central block IAB donor. This means the algorithm effectively accounts for the overload in the TA process, improving QoS for passengers by ensuring more resources are available in its serving IAB donor.

#### *B.2 Transmission Buffer Load*

In Fig. 4, we present the time evolution of the amount of buffered bits in different nodes in the system: bits in mIAB MT (dotted curves), IAB donors (solid curves) and mIAB DU (dashed curves). The curves for standard solution and proposed solutions are represented by blue and red curves, respectively.

Focusing firstly in the UL backhaul, i.e., mIAB MT, we can see that our proposed solution results in a significantly lower accumulation of buffered bits, especially halfway through the simulation, when the bus is closer to the central IAB donor, as expected, since the connection between the mIAB node and the overloaded IAB donor is prevented. When the DL access and backhaul at IAB donors are regarded, we can also observe a lower bits accumulation for our proposed solution. However, the decrease in buffer accumulation with our proposal compared to the standard solution is not at the same level as in UL backhaul mIAB MT. The reason is that interference becomes more critical in the DL when the bus passes in front of the second block, since the closest IAB donor (the one at the central block) providing the highest RSRP becomes a major source of interference to the backhaul in DL. This higher interference leads to lower throughput that causes queuing levels to increase.

Fig. 4 also shows the number of bits at the DL access of mIAB DU. Interestingly, the load accumulation, in this case,

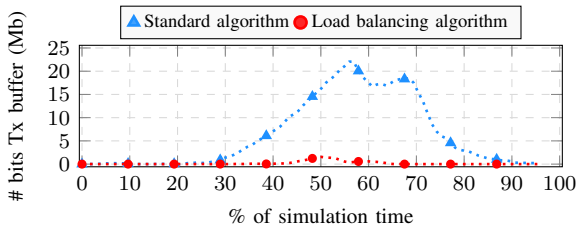


(a) Buffered bits to be sent in UL by mIAB MT (backhaul).

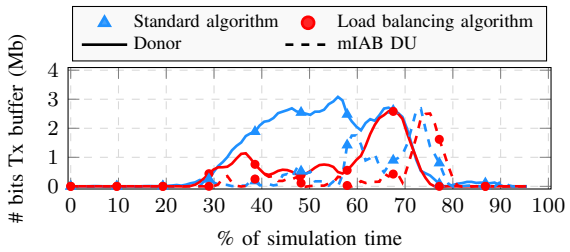


(b) Buffered bits to be sent in downlink (DL) by IAB donors to mIAB links (solid) and by mIAB to passengers links (dashed).

Fig. 4: Buffered bits (in Mb) to be sent in UL by mIAB MT (backhaul) (dotted), by IAB donors to mIAB links (solid), and by mIAB to passengers links (dashed).

takes place mainly during the last part of the simulation. This happens because after the bus passes through the second block, it finally connects to the rightmost IAB donor which has more resources to serve it in the DL backhaul. Then, the rightmost IAB donor starts to send the packets that where previously clogged in the overloaded IAB donor (in the central block), which in turn overloads temporarily the mIAB node buffer. We can also see that when using Algorithm 1, the buffer size accumulation is lower at first but becomes higher during 70% to 80% of the simulation time.

#### *B.3 UL Throughput*

In Fig. 5, we present the cumulative distribution function (CDF) of passengers (solid curves) and pedestrian (dashed curves) UL throughput for the proposed (red curves) and standard solutions (blue curves). For passengers, the proposed solution shows throughput gains over the standard solution. At the $90^{\text{th}}$ percentile, the throughput for the proposed and standard solutions are of 5.63 Mbps and 5.11 Mbps, respectively, which leads to a performance gain of approximately 10%. For the $10^{\text{th}}$ percentile, the performance gain is more modest (2.3%). Considering the passenger and pedestrian throughputs, there is a net loss of 1.9% at the $90^{\text{th}}$ percentile, and a small gain of 0.13% at the $10^{\text{th}}$ percentile. The gains were more prominent in the higher percentiles due to, e.g., the random nature of the pedestrian positioning, which may cause them to become closer to the mIAB node causing more interference in some iterations of the simulation.

For pedestrians, note that our proposal leads to a slight throughput degradation in the highest percentiles. The reason for this is that the proposed solution connects the mIAB node with the less overloaded IAB donors for a longer time. Thus, the pedestrians from these IAB donors, which have the highest throughputs (highest percentiles in the plot), have to share radio resources with the mIAB node leading to a

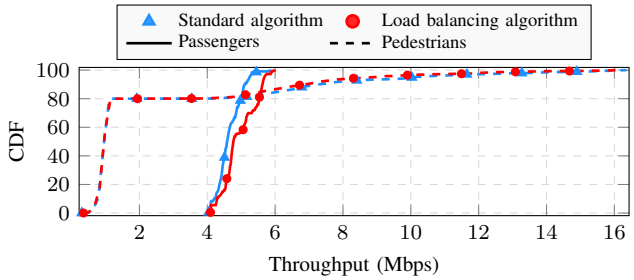


Fig. 5: UL throughput CDF for the two studied topology adaptation algorithms.

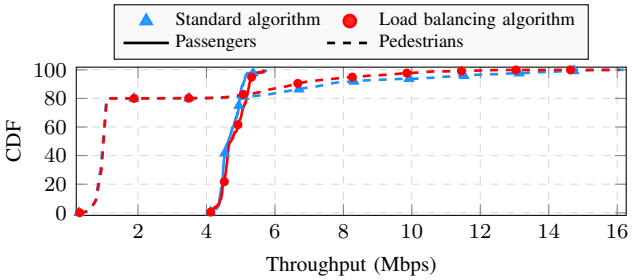


Fig. 6: DL throughput CDF for the two studied topology adaptation algorithms.

throughput degradation. For the same reason, we would expect a throughput improvement for pedestrians at the central block (lower percentiles in the plot) with the proposed solution compared to the standard one. However, as there are too many pedestrians to share the system resources in this block, the throughput improvement is not noticeable.

### *B.4 DL throughput*

In Fig. 6, we present the CDF of passengers (solid curves) and pedestrian (dashed curves) DL throughput for the proposed (red curves) and standard solutions (blue curves). We can see that there was a general improvement in QoS for passengers, but not as expressive as for the UL scenario. While in the 90$^{th}$ percentile the proposed solution achieves a performance gain of 3.3%, no performance gain can be seen in the 10$^{th}$ percentile. These lower gains in DL throughput for passengers can be explained by the increased backhaul interference the mIAB node experiences, particularly when it passes in front of the overloaded IAB donor (as previously explained).

For pedestrians, the performance of the proposed and standard solutions are very similar, except at the higher percentiles where our solution presents a performance loss of 13% at the 90$^{th}$ percentile and a net loss of 6.3%. There is a small net benefit of 0.07% at the 10$^{th}$ percentile. The reason is the same as stated for the UL performance in Fig. 5: with the proposed solution, the less loaded IAB donors have to share their resources for a longer time with the mIAB node which leads to performance degradation for the pedestrians with higher throughputs. Despite this performance loss, the throughput of 6.67 Mbps achieved at the 90$^{th}$ percentile for the proposed solution is still considered a good QoS for mobile applications.

## VI. Conclusions

This work investigated and compared a standard RSRP-only based TA algorithm with a proposed solution that additionally takes into account the load in the network nodes. Based on our analyses, the proposed solution significantly reduced the amount of buffered bits, outperforming the standard solution in terms of throughput for passengers. Our proposed solution negatively affected the performance of pedestrian UEs, but mostly the ones with over provision of QoS. Therefore, the proposed solution effectively enhances the overall QoS for passengers without significantly compromising the performance of pedestrians.

## References

[1] R. Flamini, D. De Donno, J. Gambini, *et al.*, "Towards a heterogeneous smart electromagnetic environment for millimeter-wave communications: An industrial viewpoint," *IEEE Trans. Antennas Propag.*, vol. 70, no. 10, pp. 8898–8910, Feb. 2022. DOI: 10.1109/TAP.2022.3151978.

[2] R. A. Ayoubi, M. Mizmizi, D. Tagliaferri, D. D. Donno, and U. Spagnolini. "Network-controlled repeaters vs. reconfigurable intelligent surfaces for 6G mmW coverage extension." arXiv: 2211.08033. (Nov. 2022).

[3] M. Polese, M. Giordani, T. Zugno, *et al.*, "Integrated access and backhaul in 5G mmWave networks: Potential and challenges," *IEEE Commun. Mag.*, vol. 58, no. 3, pp. 62–68, Mar. 2020. DOI: 10.1109/MCOM.001.1900346.

[4] C. Madapatha, B. Makki, C. Fang, *et al.*, "On integrated access and backhaul networks: Current status and potentials," *IEEE Open J. Commu. Soc.*, vol. 1, pp. 1374–1389, Sep. 2020. DOI: 10.1109/OJCOMS.2020.3022529.

[5] V. F. Monteiro, F. R. M. Lima, D. C. Moreira, *et al.*, "TDD frame design for interference handling in mobile IAB networks," in *Proc. of the IEEE Global Telecommun. Conf. (GLOBECOM)*, Dec. 2022, pp. 5153–5158. DOI: 10.1109/GLOBECOM48099.2022.10001454.

[6] O. Teyeb, A. Muhammad, G. Mildh, E. Dahlman, F. Barac, and B. Makki, "Integrated access backhauled networks," in *Proc. of the IEEE Vehic. Tech. Conf. (VTC)*, Honolulu, HI, USA, Nov. 2019, pp. 1–5. DOI: 10.1109/VTCFall.2019.8891507.

[7] 3GPP, "Study on vehicle-mounted relays; stage 1 (release 18)," 3rd Generation Partnership Project (3GPP), TR 22.839, Sep. 2021, v.18.0.0. [Online]. Available: http://www.3gpp.org/ftp/Specs/html-info/22839.htm (visited on 10/20/2021).

[8] 3GPP, "NR; study on integrated access and backhaul (release 16)," 3rd Generation Partnership Project (3GPP), TR 38.874, Dec. 2018, v.16.0.0. [Online]. Available: http://www.3gpp.org/ftp/Specs/html-info/38874.htm (visited on 04/13/2021).

[9] V. F. Monteiro, F. R. M. Lima, D. C. Moreira, *et al.*, "Paving the way towards mobile IAB: Problems, solutions and challenges," *IEEE Open J. Commu. Soc.*, vol. 3, pp. 2347–2379, Nov. 2022. DOI: 10.1109/OJCOMS.2022.3224576.

[10] M. Choi and H. Chung, "Relay node load balancing method in mobile communication environment," in *Proc. of the IEEE Internat. Conf. on Information and Communication Technology Convergence*, 2021, pp. 1–3. DOI: 10.1109/ICTC52510.2021.9620816.

[11] Q.-H. Tran, T.-M. Duong, and S. Kwon, "Load balancing for integrated access and backhaul in mmwave small cells," *IEEE Access*, vol. 11, pp. 138 664–138 674, Dec. 2023. DOI: 10.1109/ACCESS.2023.3338567.

[12] 3GPP, "NR; NR and NG-RAN Overall description; Stage 2," 3rd Generation Partnership Project (3GPP), TS 38.300, Jul. 2020, v.16.2.0. [Online]. Available: http://www.3gpp.org/ftp/Specs/html-info/38300.htm (visited on 04/13/2023).

[13] P. Agyapong *et al.*, "Simulation guidelines," METIS, Deliverable 6.1, Oct. 2013. [Online]. Available: https://metis2020.com/wp-content/uploads/deliverables/METIS_D6.1_v1.pdf (visited on 09/20/2021).

[14] Y. Sui, I. Guvenc, and T. Svensson, "Interference management for moving networks in ultra-dense urban scenarios," *Journal of Wireless Commun. and Netw.*, vol. 111, pp. 1–32, Apr. 2015. DOI: 10.1186/s13638-015-0326-1.

[15] 3GPP, "Study on channel model for frequencies from 0.5 to 100 GHz," 3rd Generation Partnership Project (3GPP), TR 38.901, Sep. 2017, v.14.2.0. [Online]. Available: http://www.3gpp.org/DynaReport/38901.htm (visited on 09/26/2017).

[16] A. M. Pessoa, I. M. Guerreiro, C. F. M. e Silva, *et al.*, "A stochastic channel model with dual mobility for 5G massive networks," *IEEE Access*, vol. 7, pp. 149 971–149 987, Oct. 2019, ISSN: 2169-3536. DOI: 10.1109/ACCESS.2019.2947407.

[17] 3GPP, "Study on evaluation methodology of new vehicle-to-everything (V2X) use cases for LTE and NR," 3rd Generation Partnership Project (3GPP), TS 37.885, Dec. 2018, v.15.2.0. [Online]. Available: http://www.3gpp.org/ftp/Specs/html-info/37885.htm (visited on 04/17/2019).